Bunch Compression for a Short-Pulse Mode in Cornell's ERL

Joel R. Thompson
Cornell University, Ithaca, New York 14853

April 24, 2009

Abstract

The production of ultra-short x-rays in Cornell's Energy Recovery Linac (ERL) requires electron bunch lengths of less than 100fs with minimal transverse emittance growth and energy spread. Because the linac consists of two sections separated by an arc, CSR forces limit the bunch length in the linac, and bunch compression has to be done after acceleration. Creation of such short bunches requires a second order bunch compression scheme with correction of the third order dispersion. In this paper, we discuss possible bunch compression systems and explore the benefits of each using the tracking program TAO, including CSR forces. Overall, we find that a FODO compressor utilizing dipole, quadrupole and sextupole magnets can best achieve the design goals of the short pulse mode.

1 Introduction

Bunch compression is achieved, for relativistic particles, by introducing a correlation between the time of flight of a section of the bunch and its energy. This works by first utilizing RF cavities to introduce longitudinal energy spread along the bunch and then sending the bunch through a dispersive beam line. The dispersive beam line introduces the desired correlation between energy and time of flight. Typically, the parts of the beam with higher energy have a shorter time of flight. By choosing the appropriate dispersive

section, we can cause the head and tail of the bunch to move closer together, thereby reducing the bunch length.

In order to achieve ultra short bunches as required in Cornell's ERL short pulse mode, one must design a compressor with relatively large transport terms, T_{56} and T_{566}. Also, in order to avoid transverse emittance growth due to CSR in the turn around section, we must compress after the second linac, where the beam energy is large. Achieving large transport terms while limiting emittance growth requires a bunch compressor with at least four, independently controllable parameters. In this paper, we utilize the simulation program TAO to show that a FODO compressor utilizing dipole, quadrapole, and sextupole magnets can achieve the design goals of short pulse mode in the ERL, even when the effects of CSR are taken into account.

2 Bunch Compression

Bunch compression requires at least two steps. The first is to introduce a correlation between the energy and longitudinal position of the particles in the bunch. This is most easily achieved by accelerating the bunch slightly off crest in RF cavities. Since acceleration has no effect on the longitudinal position of each particle (with respect to the bunch center) we can describe the acceleration by the following set of equations.

$$E_{f,j} = E_{i,j} + \Delta E \cos(\phi + \frac{\omega}{c} z_j), \quad (1)$$

$$z_{f,j} = z_{i,j}, \quad (2)$$

where $\Delta E = eV_{RF}$, ω is the angular RF frequency, c is the speed of light and j is the particle index. It is important to note that a positive z_j represents a particle that is ahead of the reference particle; that is, a particle at the head of the bunch. The second step of bunch compression is to introduce a correlation between the energy and the time of flight of particles in the bunch. In this way, one can convert the energy spread introduced by acceleration into a decrease in bunch size. Perhaps the simplest way to achieve this is through the relationship between energy and velocity. Classically, a larger energy necessarily implies a larger velocity, which implies a shorter time of flight. Therefore, if an electron bunch behaved classically, one would expect the section of the bunch with the higher energy to effectively move forward in phase space. If one chooses the acceleration phase properly so that the tail of

the bunch has the largest energy, we then expect the phase space distribution to shear as it propagates, allowing for compression. However, an electron in an accelerator is very relativistic and so its velocity is always approximately c, regardless of its energy. Therefore, we must introduce a correlation between energy and time-of-flight in some other way, as described below.

2.1 Dispersion

The linear equation of transverse motion for a particle traveling through a magnetic structure in an accelerator is

$$x''(s) + \left[\kappa^2(s) + k(s)\right] x(s) = \kappa(s)\delta, \tag{3}$$

where $\delta \equiv \frac{E_j - E_0}{E_0}$, E_0 is the energy of the reference particle, x is the transverse direction, s is the position along the orbit, κ is the dipole strength, and k is the quadrapole strength. So, the transverse position is dependent upon the energy of the electron. Typically, one defines the dispersion function, $D(s)$, as the transverse trajectory for a particle with $\delta = 1$. That is,

$$D''(s) + \left[\kappa^2(s) + k(s)\right] D(s) = \kappa(s). \tag{4}$$

As this is an inhomogeneous differential equation, it follows that the trajectory of an off energy particle is given by

$$x(s) = x(s)_{\delta=0} + D(s)\delta, \tag{5}$$

where $x(s)_{\delta=0}$ is the trajectory of a particle with the design energy. Eq. 4 is only a linear approximation of a more general non-linear differential equation which describes the transverse motion of a particle through an accelerator. In general one may start with this nonlinear equation of motion and following similar steps write

$$x(s) = x(s)_{\delta=0} + T_{16}\delta + T_{166}\delta^2 + ..., \tag{6}$$

where $T_{16} \equiv D(s)$, T_{166} is the second order dispersion, etc. One calls the trajectory described by $x(s)_{\delta=0}$ the betatron trajectory. In general the difference in transverse position between an off energy particle and the on energy particle, $\Delta x \equiv x(s) - x(s)_{\delta=0}$, will lead to a difference in the time of

flight between the particles. For convenience we assume a coordinate system that moves with the reference particle (a particle with $x = 0$). That is, $x(s)_{\delta=0} = 0$ and $\Delta x = x(s)$. This convention will be used throughout the rest of the paper.

The longitudinal position of a particle in a dispersive section is dependent upon Δx and therefore dependent upon the energy of the particle. Assuming that the j_{th} particle has some initial longitudinal position of $z_{i,j}$ with respect to the reference particle, we can write

$$z_{f,j}(s) = z_{i,j}(s) + T_{56}\delta_j + T_{566}\delta_j^2 + ..., \tag{7}$$

with yet undetermined constants T_{56}, T_{566},... In a dispersive section particles with different energies will follow different paths and therefore have different path lengths. If the difference in path length between the j_{th} particle and the reference particle is ΔL then the longitudinal position of the j_{th} particle after is passes through a dispersive section is

$$z_{f,j}(s) = z_{i,j}(s) + \Delta L \tag{8}$$

Assuming only motion in the x-z plane, the path length of a trajectory is given by

$$|dr| = \sqrt{(1 + \kappa x)^2 + x'^2}dl. \tag{9}$$

So, the difference in longitudinal position with respect to the reference particle at position L is given by

$$\Delta z = \int_0^L \{1 - \sqrt{(1 + \kappa x)^2 + x'^2}\}dl. \tag{10}$$

Using both Eq. 6 and Eq. 7 and expanding to second order in δ we find

$$T_{56}\delta + T_{566}\delta^2 = -\delta \int_0^L \kappa T_{16} dl - \delta^2 \int_0^L [\kappa T_{166} + \frac{1}{2}T_{16}'^2 + \frac{1}{2}(\kappa T_{16})^2]dl, \tag{11}$$

which implies that

$$T_{56} = -\int_0^L \kappa T_{16} dl, \tag{12}$$

and it can be argued that to a good approximation [2]

$$T_{566} \approx -\int_0^L \kappa T_{166} dl. \tag{13}$$

The above analysis implies that we can accomplish the second step of bunch compression by sending a bunch through a dispersive section. In the next section we will use these ideas to discuss the basics of first and second order compression.

2.2 First Order Bunch Compression

The simplest method to decrease the longitudinal extension of a bunch is via first order compression. This scheme is termed first order compression because it ignores all nonlinear terms in Eq. 7. That is, we assume for the bunch compressor

$$E_f = E_0, \tag{14}$$
$$z_f = z_i + T_{56}\delta_f. \tag{15}$$

Assuming that the bunch is accelerated with a negative phase, we expect the head of the bunch to have a higher energy than the tail. Now, for $T_{56} < 0$, Eq. 15 indicates that particles with a higher energy will move backward with respect to the reference particle and particles with a lower energy will move forward with respect to the reference particle. So the head of the bunch will move backward and the tail of the bunch will move forward, which will provide us with the decrease in the longitudinal extension that we desire. In order to determine the T_{56} that gives the shortest bunch length, we choose the T_{56} that gives $z_f = 0$ to first order in z. Combining Eq. 2 and Eq. 15 we find

$$z_{f,j} = z_{i,j} + T_{56}\frac{E_{i,j} - E_{i,0} + \Delta E\{\cos(\phi + kz_{i,j}) - \cos(\phi)\}}{E_{f,0}} \tag{16}$$

If we assume no initial energy spread and expand to first order in $z_{f,i}$ we find that

$$z_{f,j}^{(1)} = z_{i,j} - T_{56}\frac{\Delta E \sin(\phi) k z_{i,j}}{E_{f,0}}. \tag{17}$$

Now to compress to first order we must set $z_{f,j}^{(1)}$ to zero. Which implies that

$$T_{56} = \frac{E_{f,0}}{E_{f,0} - E_{i,0}} \frac{1}{k \tan(\phi)} \tag{18}$$

It is important to realize that in choosing the above T_{56} we are removing all linear dependence on z in the post compression phase space. Therefore we expect the post-compression phase space to display an essentially parabolic shape. This characteristic C shape is shown in Fig. 1 c). In order to compress the bunch further we can correct to first and second order in z_f. To achieve this we must take into account the second order z dependence on energy as well. That is, we must include the T_{566} term in our expansion.

2.3 Second Order Bunch Compression

In a second order compression scheme we begin with

$$\begin{aligned} E_f &= E_0, & (19)\\ z_f &= z_i + T_{56}\delta_f + T_{566}\delta_f^2. & (20) \end{aligned}$$

Notice that if $T_{566} < 0$, the second order term acts to move the front and back of the bunch towards the reference particle. This is exactly the type of motion we need to remove the C shape characteristic of first order compression. In this compression scheme we demand that z_f is zero to both first and second order in z. To second order in z, we can write the energy as

$$\delta = \frac{\Delta E}{E_{f,0}}\{-\cos(\phi)\frac{k z_{i,j}^2}{2} - \sin(\phi) k z_{i,j}\} \tag{21}$$

Now plugging into Eq. 20 and keeping both 1_{st} and 2_{nd} order terms we find,

$$z_{f,j}^{(1)} = z_{i,j} - T_{56}\frac{\Delta E \sin(\phi) k z_{i,j}}{E_{f,0}}, \tag{22}$$

$$z_f^{(2)} = -T_{56}\frac{\Delta E}{E_{f,0}}\cos(\phi)\frac{(kz_{i,j})^2}{2} + T_{566}\frac{\Delta E^2}{E_{f,0}^2}\sin^2(\phi)(kz_{i,j})^2. \tag{23}$$

Setting these equal to zero we find,

$$T_{56} = \frac{E_{f,0}}{E_{f,0} - E_{i,0}}\frac{1}{k\tan(\phi)}, \tag{24}$$

$$T_{566} = \frac{E_{f,0}}{E_{f,0} - E_{i,0}}\frac{T_{56}}{2\tan^2(\phi)}. \tag{25}$$

We can then define

$$r \equiv \frac{T_{566}}{T_{56}} = \frac{E_{f,0}}{E_{f,0} - E_{i,0}}\frac{1}{2\tan^2(\phi)}. \tag{26}$$

It is important to note that in order to get rid of the second order curvature we need a T_{566} with the same sign as T_{56}, which implies that $r > 0$. Fig. 1 illustrates the second order compression scheme. Notice that after 2_{nd} order compression the phase space displays an "S" like shape. This is expected because we have corrected to third order and therefore expect z^3 terms to be the dominant terms. The "S" like phase space distribution is essentially a z^3 plot rotated by 90^O. It is possible to use a similar analysis to correct for the third order terms by introducing a T_{5666} term. But typically this is unnecessary as a second order compression scheme provides sufficient bunch compression. In our case, second order compression is sufficient.

3 ERL Bunch Compressor

Producing very short, relatively coherent x-rays in the ERL requires very short bunches with a relatively small energy spread. As we increase the accelerating phase, the post-acceleration longitudinal phase space becomes more linear and therefore has smaller higher order components. Therefore second order compression is more effective at a larger accelerating phase.

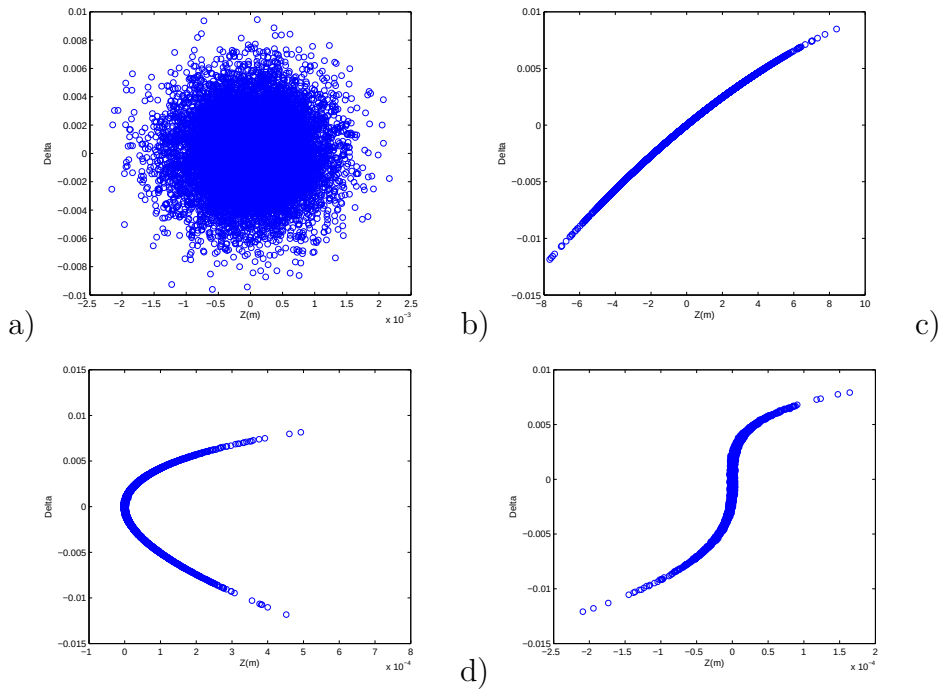

Figure 1: a) Pre-acceleration, pre-compression bunch phase space plot for Gaussian distribution b) Post-acceleration, pre-compression bunch phase space plot. c) Post-acceleration, post-compression bunch phase space plot for 1st order compression scheme. d) Post-acceleration, post-compression bunch phase space plot for 2nd order compression scheme.

Table 1: ERL Compressor Design Parameters

RF Frequency	1.3GHz
Initial Energy	10MeV
Final Energy	5GeV
Initial Bunch Length	2 ps
Final Bunch Length	100 fs
Initial Normalized Horizontal Emittance	5×10^{-6} m
Initial Normalized Vertical Emittance	5×10^{-6} m
Final Normalized Horizontal Emittance	$< 1 \times 10^{-5}$ m
Final Normalized Vertical Emittance	$< 1 \times 10^{-5}$ m
Final RMS Energy Spread	$< 3 \times 10^{-3}$

Eq. 2 indicates that a source of energy spread increase is acceleration. So, one can achieve a very small bunch length by increasing the accelerating phase, but at the cost of increasing energy spread. Eq. 25 also indicates that as one decreases the accelerating phase, the magnitude of the optimal T_{56} and T_{566} will increase. As we will see shortly, compressors with large T_{56} and T_{566} values are difficult to design and typically require very strong, and therefore costly, magnets. In the following we will discuss the pros and cons of different bunch compressor designs. Table 1 shows the design goals of the ERL bunch compressor.

3.1 Compressor Design Considerations

In order to compress to second order we must be able to vary T_{56} and T_{566} independently and maintain an $r > 0$. In order to prevent emittance growth over the length of the compressor both the slope and value of the dispersion function need to be zero to all orders at the end of the compressor. If the dispersion and its derivative are not zero at the end of the bunch compressor then the transverse equation for off energy particles is given by

$$x(s) = T_{16}\delta + T_{166}\delta^2 + ..., \tag{27}$$

$$x'(s) = T'_{16}\delta + T'_{166}\delta^2 + ... \tag{28}$$

Particles with non zero δ will be translated in transverse phase space by an amount dependent on their energy. This translation leads to an increase in

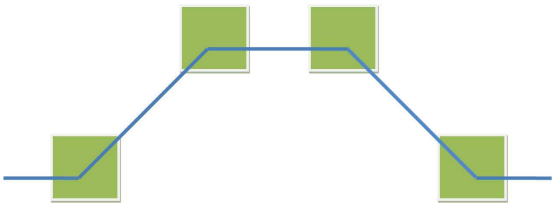

Figure 2: Schematic of chicane bunch compressor.

the phase space area occupied by the particles and therefore leads to a growth in the transverse emittance. In order to prevent emittance growth, we force $x(s) = 0$ and $x'(s) = 0$ which implies that $T_{16} = T'_{16} = T_{166} = T'_{166} = ... = 0$. Typically, only very special compressor designs have the symmetry for the dispersion to be corrected to all orders. We will generally assume that the majority of the emittance growth is due to uncorrected first, second and third order dispersions and only require that these dispersions are fully corrected at the end of the compressor.

3.2 Chicane Compressor

Perhaps the simplest compressor design is the so called chicane compressor. This compressor is shown in Fig. 2. The chicane compressor consists of only four rectangular dipole magnets arranged in a mirror symmetric way about the center, with the middle two magnets having an equal but opposite dipole strength of the outer two.

The chicane compressor is one of the few compressor designs where the dispersion is automatically corrected to all orders. This automatic correction is due to the mirror symmetry of the design and the fact that only rectangular bend magnets are used. The automatic dispersion correction and simplicity of the structure makes the chicane a very desirable compressor design. Unfortunately, the chicane compressor has an r value which is fixed and negative, not positive and variable as required. To show this we start with the standard differential equations of the first and second order dispersion functions.

$$T''_{16}(s) + (\kappa^2(s) - k(s))T_{16}(s) = \kappa(s), \tag{29}$$

$$T''_{166}(s) + (\kappa^2(s) - k(s))T_{166}(s) = f^{(2)}, \tag{30}$$
$$\tag{31}$$

where

$$f^{(2)} = -\kappa(s)\left[1 - \frac{1}{2}{T'_{16}}^2 - \kappa T_{16}(s)(2 - \kappa(s)T_{16})\right] + k(s)T_{16}(1 - 2\kappa(s)T_{16}) - \frac{1}{2}m(s)T_{16}^2, \tag{32}$$

and m is the sextupole strength. For the case of a chicane structure all magnet strengths except the dipole are zero. Therefore, the dispersion differential equations become

$$T''_{16} + \kappa^2(s)T_{16} = \kappa, \tag{33}$$
$$T''_{166} + \kappa^2(s)T_{166} = -\kappa\left[1 - \frac{1}{2}T'^2_{16} - \kappa T_{16}(2 - \kappa T_{16})\right]. \tag{34}$$

It can be shown that for dipoles of average strength it is roughly true that [2]

$$T''_{166} + \kappa^2 T_{166} \approx -\kappa \tag{35}$$

and therefore T_{166} follows $-T_{16}$. So, together with Eq. 12 and Eq. 13 this result implies that $\frac{T_{566}}{T_{56}} < 0$. Also, note that the shape of both dispersion functions only depends on κ and therefore T_{56} and T_{566} only depend on κ. That is, we can not vary T_{56} and T_{566} independently as required. However, we can modify the chicane compressor to have independent T_{56} and T_{566} values by adding sextupole magnets. This modified chicane compressor is described in the next section.

3.3 Modified Chicane Compressor

The modified chicane compressor is a simple chicane compressor with sextupole magnets placed in between each dipole magnet. The sextupole strengths are chosen in a mirror symmetric way (i.e. the outer sextupoles are of equal strength).

The sextupole magnets allow one to vary T_{56} independently of T_{566}. This can be shown by examining Eqs. 29 and 30 for the case with only dipole and sextupole magnets. We find that

$$T''_{16} + \kappa^2(s)T_{16} = \kappa, \tag{36}$$

$$T''_{166} + \kappa^2(s)T_{166} = -\kappa\left[1 - \frac{1}{2}T'^2_{16} - \kappa T_{16}(2 - \kappa T_{16})\right] - \frac{1}{2}mT^2_{16}. \tag{37}$$

Together with Eq. 12 and Eq. 13, these imply that T_{56} is a function of dipole strength and T_{566} is a function of both dipole and sextupole strength. Therefore, by varying the strength of the sextupoles we can vary T_{566} independently of T_{56}. This simple argument also indicates that the first order dispersion of the modified chicane compressor is identical to that of the chicane compressor. That is, the slope and value of the first order dispersion is automatically corrected. As higher order dispersions depend on the sextupole strength, only the first order dispersion remains automatically corrected. The modified chicane compressor permits correction of the second order dispersion by varying the strength of the center sextupole until the second order dispersion slope is zero at the compressor symmetry point. So, the modified chicane compressor permits correction of both the first and second order dispersion at the end of the compressor. Unfortunately, since higher order dispersions are no longer corrected, we expect significant emittance growth. The majority of this emittance growth is due to uncorrected third order dispersion and related to both the value of the third order dispersion and Twiss parameters at the end of the compressor. In order to minimize the final emittance, we must minimize the third order dispersion at the end of the compressor. In specifying the T_{56} and T_{566} values and correcting the first and second order dispersion, we have effectively set the strengths of all magnets in the compressor. Therefore, the only free parameters left to vary are the lengths of the magnets and drift sections and the initial Twiss parameters. In the following a simplified argument, we exactly derive an expression relating the final emittance to the length of the compressor and Twiss parameters.

In order to determine the relationship between the length of compressor and the third order dispersion we need to determine the value of the dispersion at each point along the compressor. In the following explanation we will adopt the convention that the superscript denotes the specified element and all dispersions are calculated at the center of the element. For example, $T^(1)_{16}$ indicates the value of the first order dispersion at the center of the

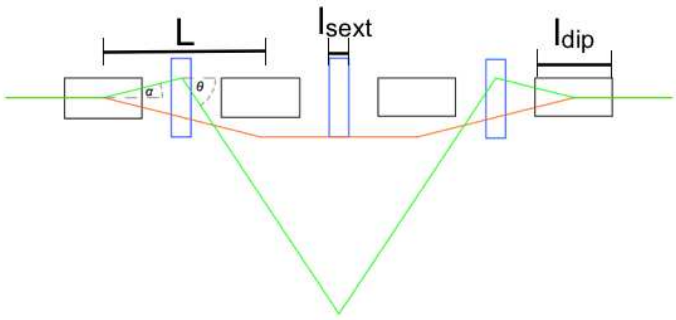

Figure 3: Layout of Modified Chicane Compressor. The black rectangles represent rectangular bend magnets and the blue rectangles represent sextupole magnets. Orange lines represent first order dispersion, T16, and green lines represent second order dispersion, T166.

first element (first dipole) and $T^(2)_{16}$ would indicate the value at the center of the second element (first sextupole). A diagram of the modified chicane compressor is shown in Fig. 3.

The dispersion differential equations for the modified chicane compressor are given by

$$T''_{16} + \kappa^2(s)T_{16} = \kappa \tag{38}$$

$$T''_{166} + \kappa^2(s)T_{166} \approx -\kappa - \frac{1}{2}m(s)T^2_{16} \tag{39}$$

$$T''_{1666} + \kappa^2(s)T_{1666} \approx \kappa + \frac{1}{2}m(s)T^2_{16} + m(s)T_{16}T_{166} \tag{40}$$

It is clear from these equations that before the first sextupole $T_{16} \approx -T_{166} \approx T_{1666}$. If we assume that the first dipole is sufficiently weak such that $\kappa^2 T_{16} << \kappa$, we find that $T'^{(1)}_{16} \approx \kappa l_{dip} \equiv \alpha$. Moreover, the value of T'_{16} remains unchanged until the second dipole magnet, where $T'_{16} = 0$. Therefore, we can calculate the first order dispersion at the first and second sextupoles and second dipole.

$$T^{(2)}_{16} = \alpha L/2 \tag{41}$$

$$T^{(3)}_{16} = \alpha L \tag{42}$$

$$T^{(4)}_{16} = \alpha L \tag{43}$$

$T'_{16} \approx \alpha \approx -T'_{166} \approx T'_{1666}$ before the first sextupole. Now, examining Eq. 40, we see that after the first sextupole the slope of T_{166} changes by $-\frac{1}{2}m_1 l_{sext}(T_{16}^{(2)})^2 = -\frac{1}{8}m_1 l_{sext}\alpha^2 L^2 \equiv \theta$ and the slope of T_{1666} changes by $\frac{1}{2}m_{1sext}(T_{16}^{(2)})^2 + m_1 l_{sext}T_{16}^{(2)}T_{166}^{(2)} \approx \frac{3}{2}m_1 l_{sext}(T_{16}^{(2)})^2 = -3\theta$. Therefore, at the center of the first sextupole

$$T_{166}^{\prime(2)} = -\alpha - \frac{1}{8}m_1 l_{sext}\alpha^2 L^2 = -\alpha + \theta \tag{44}$$

$$T_{1666}^{\prime(2)} = \alpha - 3\theta \tag{45}$$

$$\tag{46}$$

Now, after the second dipole the slope of the first order dispersion must be zero. Therefore, T'_{16} must change by $-\alpha$. To a good approximation we can assume that T'_{166} and T'_{1666} change by the same amount. So at the center of the second dipole

$$T_{166}^{\prime(3)} = \theta \tag{47}$$

$$T_{1666}^{\prime(3)} = -3\theta \tag{48}$$

For the ERL compressor, we require that $T_{566} >> T_{56}$. As we will see, this implies that $\theta >> \alpha$. Therefore, we can typically ignore the effect of α on the second order dispersion and approximate it as a line with slope of θ between the first and second sextupoles (see Fig. 3). Therefore, to a good approximation

$$T_{166}^{(3)} = \theta L/2 \tag{49}$$

$$T_{166}^{(4)} = \theta L \tag{50}$$

T_{56} and T_{566} are defined as

$$T_{56} = -\int_0^L \kappa T_{16} dl \tag{51}$$

$$T_{566} \approx -\int_0^L \kappa T_{166} dl \tag{52}$$

T_{16} and T_{166} are only non-negligible at the second and fourth dipole magnets, with a value of αL and $\theta L/2$, respectively. So,

$$T_{56} = 2\alpha^2 L \Rightarrow \alpha = \sqrt{T_{56}/L} \tag{53}$$

$$T_{566} = \theta L \alpha \Rightarrow \theta = T_{566}/\sqrt{T_{56}/L} \tag{54}$$

Therefore, $\theta >> \alpha$ since $T_{566} >> T_{56}$, as expected.

In order to correct the second order dispersion, $T'_{166} = 0$ at the center of the second sextupole. From Eq. 40 we expect T'_{166} to change by $-\frac{1}{2} m_2 l_{sext} (T_{16}^{(4)})^2$ at the second sextupole. So, it must be that $-\frac{1}{2} m_2 l_{sext} (T_{16}^{(4)})^2 = -\theta$. Which implies that $m_2 l_{sext} = 2\theta/(T_{16}^{(4)})^2$. Therefore, we expect T'_{1666} to change by $\frac{1}{2} m_2 l_{sext} (T_{16}^{(4)})^2 + m_2 l_{sext} T_{16}^{(4)} T_{166}^{(4)} = \theta + 2\theta T_{166}^{(4)}/T_{16}^{(4)}$ at the second sextupole.

Plugging in for $T_{166}^{(4)}$ and $T_{16}^{(4)}$ we find that,

$$T_{1666}^{\prime(4)} = -3\theta + \theta + 2\theta\frac{\theta}{\alpha} \approx 2\theta\frac{\theta}{\alpha} \tag{55}$$

The T_{16} and T_{166} are symmetric around the center of the chicane, while the T_{1666} is not. However, all other changes in T'_{1666} will be on the order of α or θ and therefore are much smaller than the value of T'_{1666} at the center of the compressor. Therefore, T_{1666} can be approximated by a line with zero slope before the center of the second sextupole and slope of $2\theta^2/\alpha$ after it. So,

$$T_{1666}^{(7)} = 3L\theta\frac{\theta}{\alpha} \tag{56}$$

Plugging in for θ and α in terms of T_{56} and T_{566} we find that

$$T_{1666}^{\prime(7)} = \frac{2T_{566}^2}{T_{56}^{3/2}\sqrt{L}} \tag{57}$$

$$T_{1666}^{(7)} = \frac{6T_{566}^2}{T_{56}^{3/2}}\sqrt{L} \tag{58}$$

At the end of the compressor (where the slope and value of the first and second order dispersions are zero) the average emittance in the bending plane is:

$$\overline{\epsilon}^2 = \epsilon^2 + \delta^6[\gamma T_{1666}^2 + \beta {T'_{1666}}^2 + 2\alpha T_{1666} T'_{1666}] \tag{59}$$

where α, β and γ are the Twiss parameters at the end of the compressor.

Plugging in for T_{1666} and T'_{1666} we find that

$$\overline{\epsilon}^2 = \epsilon^2 + 4\delta^6 \frac{T_{566}^4}{T_{56}^3}[9\gamma L + \beta/L + 6\alpha] \tag{60}$$

In order to limit the emittance growth we must minimize this quantity. As the Twiss parameters are not the same as those predicted by linear beam dynamics because of the relatively strong sextupoles, there is no good analytical way to go about this. Rather, we use the simulation program Tool for Accelerator Optics (TAO) to find the minimum emittance by varying such quantities as magnet strength and length, while continuing to correct the first and second order dispersions and keep T_{56} and T_{566} constant. Such a minimization procedure indicates that the minimum emittance is achieved fora compressor with long and strong dipole magnets and long sextupole magnets. In practice, the strongest achievable dipole strength is about $0.05m^{-1}$. Also, by using long, strong dipoles we make a large. In order to keep the T_{56} constant, while increasing α we must decrease the overall length of the compressor. Therefore, achieving a small emittance growth necessitates a short compressor. By increasing the magnet lengths and decreasing the drift length to keep the T_{56} constant, we eventually arrive at a compressor with the shortest acceptable drift length of a few centimeters. This will be the shortest achievable compressor with the minimum possible emittance growth.

From Eq. 60 it is clear that the emittance growth scales with $T_{566}r^3$, where $r = T_{566}/T_{56}$. As both r and T_{566} increase as we decrease the accelerating phase, we generally expect the smallest emittance growth for largest accelerating phases. Of course, too large an accelerating phase will result in too large an energy spread. Therefore, we choose an accelerating phase that is just small enough to result in an energy spread just below the design value. This turns out to be 9^o. For this phase, we can choose the T_{56} so that the bunch is corrected to second order or so that the bunch length is 100 fs.

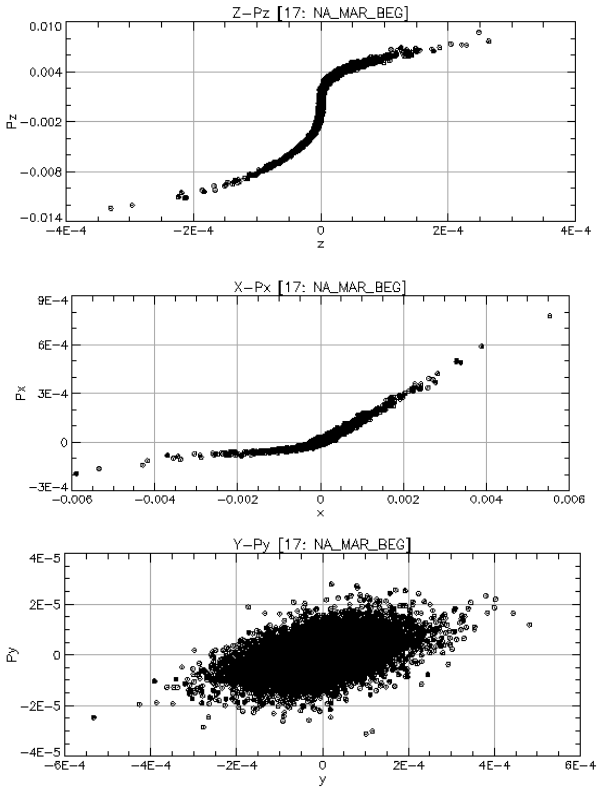

Figure 4: Post-compression phase space plots for compressed bunches in a modified chicane compressor at an accelerating phase of 9°, without CSR. Here the horizontal and vertical normalized emittances are 1.27×10^{-5} m and 5.13×10^{-6} m, respectively.

The latter method is termed undercompression and discussed later. The final minimum emittances for an optimized modified chicane compressor are given in Table 2. Phase space plots for the modified chicane compressor (ignoring CSR effects) are shown in Fig. 4. In both cases, the minimum emittance is above the ERL design value. So, while the modified bunch compressor is a short and relatively simple design, it cannot meet the ERL bunch compressor design specifications. Therefore, we must explore other designs.

3.4 FODO Compressor

The modified chicane compressor's large emittance growth was due primarily to a sharp increase in the the slope of the third order dispersion at the center sextupole. As discussed in the previous section, this increase was caused by large first and second order dispersion terms and large sextupole strength at the center sextupole. These problems can be somewhat alleviated by choosing a more "spread out" compressor design. That is, a compressor with a larger number of sextupole and dipole magnets. Such a design is the so-called FODO compressor. A layout of the FODO compressor is shown in Fig. 5. This compressor consists of a FODO lattice embedded in a chicane like structure. A FODO lattice is a series of equally spaced focusing and defocussing quadrupole magnets. These quadrupole magnets not only allow one to set up a periodic beta function, but can be varied to affect the second and third order dispersion terms. In this way, the inclusion of the quadrupole magnets adds another degree of freedom to the compressor.

Again we restrict the bending radius of all dipole magnets to be greater than 20 m and the strength of all sextupole magnets to be less than $150m^{-2}$. In order to design the most compact compressor, we choose all dipole magnets and drifts to be as short as possible. Again, we expect the third order dispersion and therefore the final normalized transverse emittance to increase as we decrease the accelerating phase. In order to compare the transverse emittance growth of the FODO compressor to that of the modified chicane compressor, we again choose a 9° accelerating phase. Post-compression phase space plots generated using TAO for the FODO compressor are shown in Fig. **??**. At 9° the final normalized emittances in the horizontal and vertical planes are 7.5×10^{-6} and 5.8×10^{-6}, respectively. Notice that the final horizontal emittance is more than 1.5 times smaller than that of the modified compressor and therefore well within the design specifications of the ERL compressor. However, when the non-linear effects of CSR are taken into account (as discussed later) the final emittance of the FODO compressor is larger than 1^{-5}. Therefore, we must modify the FODO compressor in order for it to meet the design specifications. This is discussed in the next section.

3.5 Modified FODO Compressor

In order to further decrease emittance growth we want to minimize the third order dispersion at the end of the compressor. Ideally, we would like to

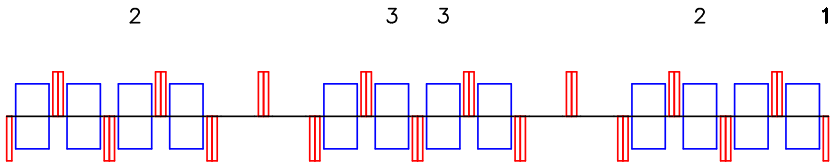

Figure 5: Layout of a FODO Bunch Compressor. Notice that the first pair of combined dipole-sextupole magnets is marked with a 2 and the second pair is marked with a 3.

correct both the slope and value of the third order dispersion at the end of the compressor by demanding that the third order dispersion slope go to zero at the center of the compressor. In specifying the T_{56} and T_{566} and demanding that the first and second order dispersion be corrected, we are effectively fixing the magnet strengths for a given compressor length. Therefore, we are still free to vary the length of each element. In designing the FODO compressor we chose the length of all magnets to be as short as possible while still keeping the strengths of each magnet within a physically reasonable range. Therefore, we are only free to vary the length of the drift elements. In the FODO design we generally require that the length of each FODO cell be identical in order to guarantee a periodic beta function. If we relax this restriction and allow varying drift lengths we can use TAO to completely correct the third order dispersion at the end of the compressor. This leads to a very small vertical emittance growth of only about 14 percent for a 9° accelerating phase. That is, the final horizontal and vertical emittances are 5.7×10^{-6} m and 5.3×10^{-6} m, respectively.

4 CSR Effects

Synchrotron radiation is emitted by any charged particle when it is accelerated by a bending magnet. This radiation is emitted mostly in a direction tangential to the curved trajectory in a bending magnet. If an ultra relativistic bunch of charged particles passes through a bending magnet, the radiation emitted in the back of the bunch can interact with the particles at the front of the bunch causing both transverse and longitudinal forces on the front of the bunch. For ultra short bunches, like those produced by the ERL bunch compressor, the wavelength of the synchrotron radiation is comparable to the length of the bunch. Therefore, the radiation emitted by the

particles at the back of the bunch is in phase, resulting in a quadratic dependence of the power emitted on the number of electrons [3]. This Coherent Synchrotron Radiation (CSR) can significantly affect both the energy spread and transverse emittances of the bunch. As the bunches produced by the ERL bunch compressor are ultra short, we expect CSR to have a significant effect. Therefore, in order to simulate the effects of CSR, we use the CSR tracking algorithm implemented in Bmad and TAO.

4.1 Undercompression

CSR effects are stronger for larger electron densities. As discussed in Sect. 2.3, bunches compressed to second order have longitudinal phase space plots that contain regions of zero curvature and infinite slope. These regions correspond to slices of the bunch with very high electron density. Therefore, we expect very strong CSR effects for fully compressed bunches. In order to minimize CSR effects we require the compressor to have a larger T_{56} term than that given by Eq. 25. This results in a more linear post-compression longitudinal phase space and therefore a bunch with lower electron density. As the name suggests, "undercompression" results in longer bunches. In order to meet the design goals given in Table 1, the final bunch length must be less than 100 fs. In order to achieve the smallest emittance growth possible, we choose the largest acceptable accelerating phase, which is again limited by the energy spread to 9°. Therefore, we "undercompress" the bunch at an accelerating phase of 9° so that it has a final bunch length of 100 fs. Fig. 6 shows phase space plots for a fully compressed bunch while Fig. 7 shows plots for an "undercompressed" bunch. Notice the dramatic difference in transverse emittance between the two. Fig. 8 shows the phase space plots for an undercompressed bunch in the modified chicane compressor with CSR. This represents the "best" case for the modified chicane compressor. Notice that the "best" case for the FODO compressor is significantly better than the modified chicane's "best" case.

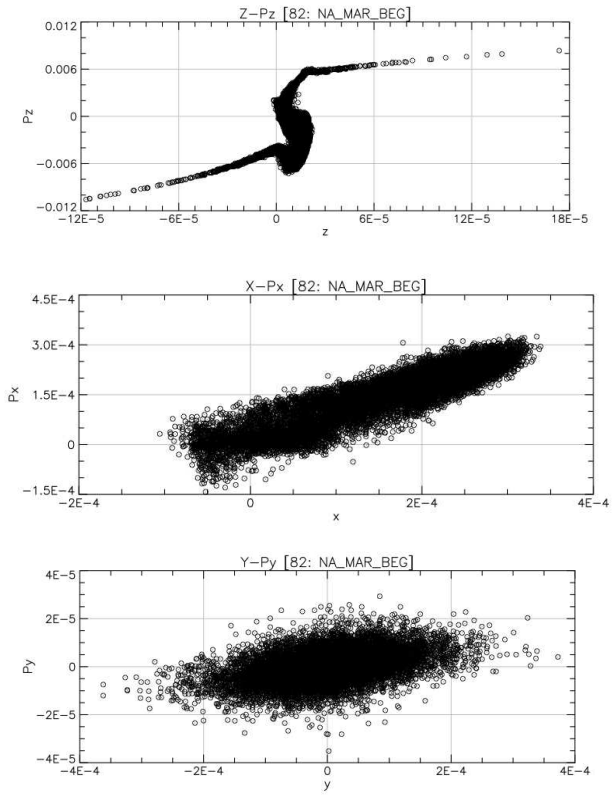

Figure 6: Post-compression phase space plots for compressed bunches in a modified FODO compressor at an accelerating phase of 9°, with CSR. Here the horizontal and vertical normalized emittances are 2.6×10^{-5} m and 5.3×10^{-6} m, respectively. Notice the relatively large CSR effects.

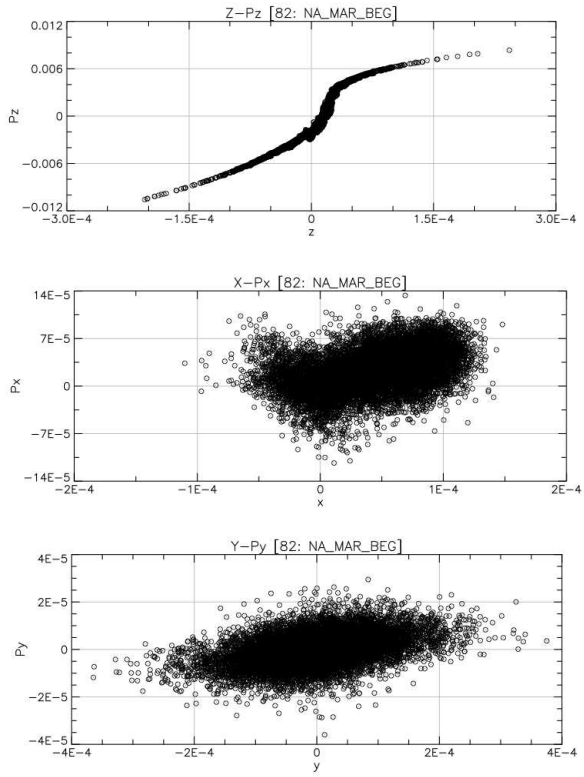

Figure 7: Post-compression phase space plots for "undercompressed" bunches in a modified FODO compressor at an accelerating phase of 9°, with CSR. Here the horizontal and vertical normalized emittances are 8.2×10^{-6} m and 5.4×10^{-6} m, respectively. "Undercompression" decreases the electron density in the bunch and therefore decreases CSR effects. Notice the relatively small emittance growth, well below the ERL design goal.

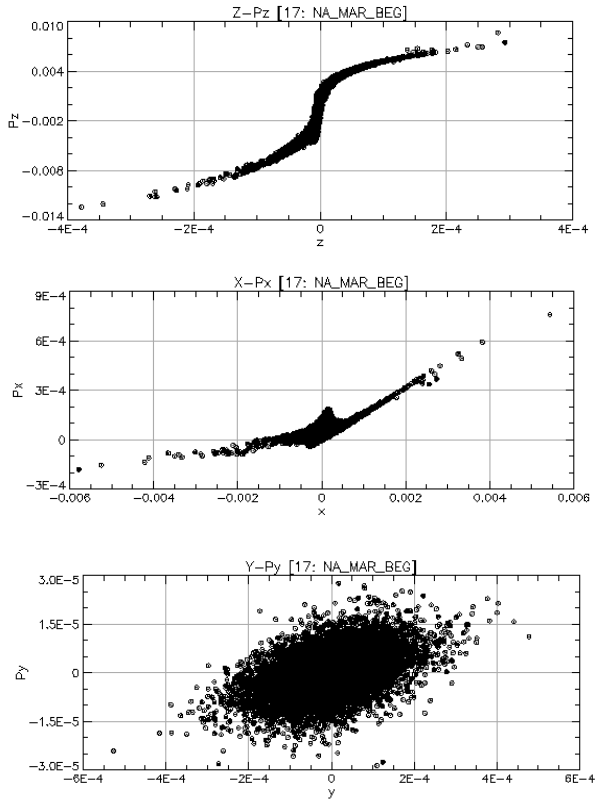

Figure 8: Post-compression phase space plots for undercompressed bunches in a modified chicane compressor at an accelerating phase of 9°, with CSR. Here the horizontal and vertical normalized emittances are 3.75×10^{-5} m and 5.35×10^{-6} m, respectively. The RMS bunch length is 100 fs and the energy spread is 2.7×10^{-3}.

Modified Chicane				
	Compressed		Undercompressed	
	No CSR	CSR	No CSR	CSR
Total Length	17.6 m	17.6 m	17.8 m	17.8 m
Bunch Length	68 fs	68 fs	100 fs	100 fs
Energy Spread	2.6×10^{-3}	3.0×10^{-3}	2.6×10^{-3}	2.9×10^{-3}
Horiz. Norm. Emitt.	1.27×10^{-5} m	5.88×10^{-5} m	1.26×10^{-5} m	3.75×10^{-5} m
Vert. Norm. Emitt.	5.13×10^{-6} m	5.36×10^{-6} m	5.33×10^{-6} m	5.35×10^{-6} m
FODO				
	Compressed		Undercompressed	
	No CSR	CSR	No CSR	CSR
Total Length	31.6 m	31.6 m	31.6 m	31.6 m
Bunch Length	58.6 fs	58.0 fs	100 fs	100 fs
Energy Spread	2.6×10^{-3}	2.8×10^{-3}	2.6×10^{-3}	2.73×10^{-3}
Horiz. Norm. Emitt.	7.25×10^{-6} m	3.06×10^{-5} m	7.44×10^{-6} m	1.25×10^{-5} m
Vert. Norm. Emitt.	6.05×10^{-6} m	6.04×10^{-6} m	6.11×10^{-6} m	6.11×10^{-6} m
Modified FODO				
	Compressed		Undercompressed	
	No CSR	CSR	No CSR	CSR
Total Length	31.3 m	31.3 m	31.3 m	31.3 m
Bunch Length	34.9 fs	37.6 fs	100 fs	96.3 fs
Energy Spread	2.6×10^{-3}	2.7×10^{-3}	2.6×10^{-3}	2.7×10^{-3}
Horiz. Norm. Emitt.	5.75×10^{-6} m	2.58×10^{-5} m	5.81×10^{-6} m	8.15×10^{-6} m
Vert. Norm. Emitt.	5.14×10^{-6} m	5.12×10^{-6} m	5.16×10^{-6} m	5.15×10^{-6} m

Table 2: End of compressor data for each of the modified compressors. Listed is data for both regular second order compression and undercompression. All data is for a 9^o accelerating phase. This is the maximum phase for which the energy spread meets the design requirements.

5 Conclusion

While the modified chicane and FODO compressors all come very close to meeting the ERL short pulse mode design goals, only the modified FODO compressor satisfies all requirements. Therefore, the FODO compressor is the best compressor for the ERL designed so far. Of course, the downside of choosing the modified FODO compressor is its relatively large length and complicated design. If one is willing to relax the stringent requirement for maximum emittance growth we could use either the shorter FODO compressor or the much shorter and simpler modified chicane. We are also currently investigating the possibility of using a simple chicane compressor and a modified turn around section in order to fully compress the bunch. In this case, we use the sextupoles in the turn around section to produce enough T_{566} before the compressor, so that the final T_{566} is exactly that required for second order compression. If this works, we will be able to achieve compression without emittance growth using a very simple compressor. However, this possibility is still being investigated. Therefore, given the current design goals, the modified FODO compressor is the best design available.

Acknowledgments

I would like to thank Prof. G.H. Hoffstaetter for his insight, direction and encouragement. Without him this project would not have been possible. I would also like to thank D. Sagan for his BMAD/TAO expertise and his help in debugging code.

References

[1] G.H. Hoffstaetter, et. al., Challenges for Beams in an ERL Extension to CESR, Proceedings EPAC08, Genoa/IT (2008)

[2] W. Decking, G. Hoffstaetter, T. Limberg, Bunch Compressor for the TESLA Linear Collider, TESLA-2000-40 (2000)

[3] D. C. Sagan, G. H. Hoffstaetter, C. E. Mayes, U. Sae-Ueng , CSR Including Shielding in the Beam, Proceedings EPAC08, Genoa/IT (2008)

[4] C. E. Mayes, G. H. Hoffstaetter, Exact 1D model for coherent synchrotron radiation with shielding and bunch compression, Physical Review ST-AB 12, 024401 (2009)

[5] K. Wille, The Physics of Particle Accelerators:An Introduction, Oxford University Press, New York (2000)

[6] H. Wiedemann, Particle Accelerator Physics II, Springer, Germany (1995)